Proceedings of the 3rd International Conference on Intelligent Cyber Physical Systems and Internet of Things (ICoICI-2025)
IEEE Xplore Part Number: CFP25VG0-ART; ISBN: 978-1-6654-5753-8

Monolithic Crystal Preclinical Tomography Detector Design with Sparse SiPM Matrix

Edward Mubanga
Department of Physics
Kapasa Makasa University
Chinsali, Zambia
edwardmubanga13@gmail.com

Davies Mubita
Deparment of physics
Mulungushi University
Kabwe, Zambia
daviesmubita@gmail.com

Ngula Walubita
Department of Information & Communication Technology
Kapasa Makasa University
Chinsali, Zambia
goodsonwalubita@gmail.com

Bibhuti Bhusan Dash
SCA, Kalinga Institute of Industrial Technology(KIIT) Deemed to be University
Bhubaneswar, India
bibhuti.dash@gmail.com

Utpal Chandra De
SCA, Kalinga Institute of Industrial Technology(KIIT) Deemed to be University
Bhubaneswar, India
deutpal@gmail.com

Sudhansu Shekhar Patra
SCA, Kalinga Institute of Industrial Technology(KIIT) Deemed to be University
Bhubaneswar, India
sudhanshupatra@gmail.com

2025 3rd International Conference on Intelligent Cyber Physical Systems and Internet of Things (ICoICI) | 978-1-6654-5753-8/25/$31.00 ©2025 IEEE | DOI: 10.1109/ICoICI65217.2025.11253192

***Abstract*— PET, Positron Emission Tomography, a cutting-edge technique, were combined in this work to produce better detector sensitivity and spatial resolution. This strategy was referred to as a dual-modality approach. PET is a cutting-edge imaging method that has completely transformed the area of medical diagnosis. With the use of this extraordinary technology, medical personnel are able to see the inner workings of the human body in real time, which provides them with crucial insights into a variety of illnesses and ailments. When PET scans are performed, just a trace quantity of radioactive material is used. A multimodal PET/SPECT detector and SiPM array that makes use of LYSO crystals was the major aim that needed to be designed and constructed. The creation of a collaborative detector that is capable of detection for both SPECT and PET modalities is presented in this paper. For the purpose of maximising the efficiency of the detector's design and evaluating its performance, Monte Carlo simulations were carried out using the program Geant4. For the purpose of the phantoms, the design was carried out in Geant4, more precisely in accordance with the NU 4-2008 standard established by the NEMA.**

***Keywords*— SPECT, Monolithic scintillator, Geant4, SiMPs, PET, Simulation with monte-carlo, National Electrical Manufacturers Association**

I. INTRODUCTION

The strategically choice of radionuclide, like technetium-99m for single-photon emission tomography (SPECT) and fluorodeoxyglucose (FDG) for positron emission tomography (PET), allows doctors to see and diagnose a variety of disorders in a non-invasive manner [1]. The invention of a multimodal PET/SPECT detector, which included a siPM along with a monolithic Lutetium Yttrium Oxyorthosilicate (LYSO) crystal, served as the foundation for this study [2]. In addition to conducting a through investigation of the SiPMs matrix LYSO monolithic scintillator, the anluysis included a detailed evaluation of the PET and SPECT detectors that are currently in use [3]. In the end, the study resulted in the successful creation of a full detector, which made use of a NEMA-Nu 2008 phantom from NEMA, as well as the calculation of attenuation lengths for PET/SPECT [4]. PET/SPECT are tomography methods used in nuclear medicine that are fundamentally different from one another in terms of the radioisotopic processes that they rely on [5]. The PET technique uses radionuclides that release positrons, such as fluorine-18. On the other hand, the SPECT technique utilises radioisotopes that generate γ-emitters, such as technetium-99m [6]. Due to the different radioisotopic characteristics of various modalities, it is necessary to utilise different detection methodologies. PET commonly employs coincidence detection, whereas SPECT utilises lead collimators to isolate γ-radiation [7,8]. Because the radiotracer that is supplied does not disrupt the biological processes that are taking place below it, this characteristic gives a considerable benefit [9]. Furthermore, the availability of a wide variety of radiopharmaceuticals that are controlled by the FDA has made it easier to build a large number of diagnostic tests for the purpose of monitoring radiolabeled cells in disease patterns and clinical tries [10]. Additionally, fluoro-2-deoxy-D-glucose, often known as FDG, is a renowned PET radiotracer that is used extensively in neurologic and oncological applications [11].

Goals

Through the use of a monolithic crystal, namely LYSO, the purpose of this investigation is to examine the application of a silicon photomultiplier (SiPM) array in order to construct a multimodal PET/SPECT detector.

Included among the secondary goals of this study are the following:

- LYSO monolithic scintillators in combination with SiPM are being evaluated as PET/ SPECT gamma cameras, while current combined PET and SPECT detectors are being reviewed and evaluated simultaneously.
- Utilising mouse phantoms for PET/SPECT analysis in order to conduct preclinical performance metrics analysis.
- Phantoms are being built inside the Geant4 framework, and simulations of the PET/SPECT detector are being performed.

The significance of this work lies in the possibility of developing detectors that are very sensible to greater radiation phases in patients across both modes (PET/SPECT). This would significantly cut down on the amount of time required for scanning and would also reduce the amount of innovative radiopharmaceuticals that are required. The significance of this finding is further highlighted by the implications it has for nuclear medicine.

Organization

The following is how the remaining article is prepared: Work relating to the previous research is included in Section II. The proposed method is presented in Section III, the experimental findings are done in Section IV, the discussion is presented in Section V, and the concluding remarks are in Section VI.

.

II. LITERRATURE SURVEY

PET/SPECT detection

PET:

PET/SPECT detection measures radioactive substances in animal tissues following injection. Scintillators record the PET detectors' LOR from gamma ray annihilation. The energy of the two photons and component particles is read by the detecting system. Annihilated photons contain energy in opposing directions and at 511 keV intervals. [12] The LOR is the result of a straight line formed by annihilation gamma ray ions. A detecting device that simultaneously captures two photon events and calculates the energy of each individual photon over a predetermined amount of time. Scintillators are utilized in PET detectors. Fig. 1 illustrates the basic principles of detection.

SPET:

SPECT imaging uses a gamma camera to capture numerous two-dimensional projections from different angles [13]. A three-dimensional set of data is produced by processing these projections using a tomographic reconstruction technique [14]. Similar to the outputs from other tomographic modalities including PET, X-ray CT, and MRI, this data collection may be analysed to produce tiny body parts along any axis [15]. Similar to PET, SPECT uses radioactive tracers and detects gamma rays. However, SPECT tracers produce measurable gamma radiation, while PET traces' positrons destroy electrons.

Many detector device employ scintillators and siPM tubes, although commercial versions use SiPMs for high resolution.

Reconstructing the PET/SPECT:

Scanning data represents input LORs. Some call these facts sinograms [16]. LORs may be configured several ways. Mental image systems depend on local and frequent mastered object examples. Rebuilding fixes this. Reconstruction may provide a 2D or 3D image of the body's radioactive atom dispersion from raw LOR data.

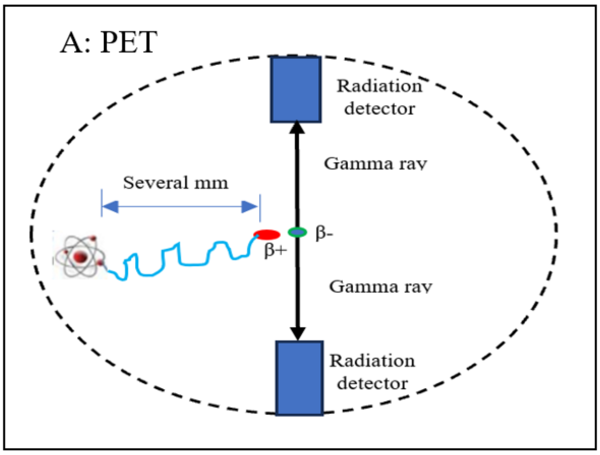

Fig. 1 (A) illustrates the basic method of detecting positron annihilation in positron emission tomography (PET). Both gamma rays are created along different pathways when the generated positron briefly moves through tissue before slowing down and colliding with an electron.

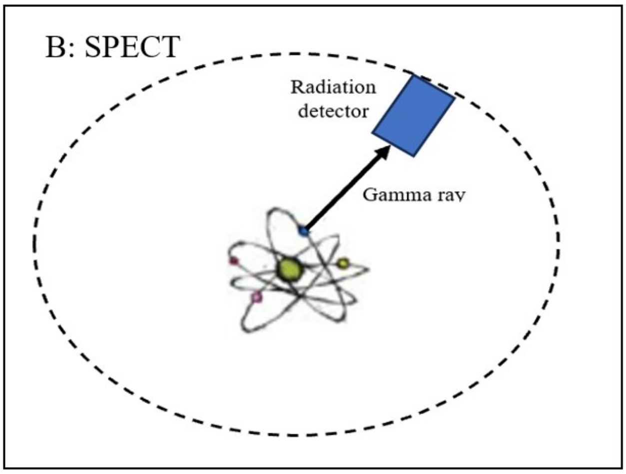

Fig. 1. (B) A rudimentary gamma camera that detects radiation

.

A mathematical representation of the obtaining mechanism is:

$$Y = J\,(a + b)$$

where "Y" stands for the gathered information (set of LORs);

J: An array of voxel probabilities is often used in the mathematical model to provide and detect LOR events;

a: The body's PET distribution for a particular pastime is unclear.

b: standardization flaws as well as the distinction between reconstructed and "actual" illustrations.

If b is 0 and the system is exclusively accessible via mathematical notions, the reconstruction's drawback might be quantitatively avoided. This change from a to Y is known as the random transformation in mathematical operations. Therefore, the change from a to Y is the inverse change of random. If b represents a fixed integer range or matrix, the reconstruction job may be addressed analytically in both situations. There are several methods for presenting analytical responses.

The most often utilised technique is filter back projection (FBP) [17]. Comparable to collecting data at the same LOR value, the FBP enabled a back projection stage that used scalar energy to integrate volume in LOR. The filtering step process accounts for non-uniform LOR spatial arrangement within a volume and eliminates superfluous sample distribution of bottom lines as well as sounds at certain frequencies.

Next are the Sheep-Logan, Hann, and Ram-Lak filters. Although computationally it provides a clear picture, they are unable to take noise dependency or certain physical quirks into consideration. Consequently, FBP will show pictures from drones. However, FBP continues to be one of the most popular reconstruction techniques due to its quick computation performance and low laptop needs. It is more reasonable to say that error d is a random price. Repeated techniques are used to solve these shortcomings.

Many redundant strategies rely on the ideal scenario and seek to function. Among the most popular styles are:

- Expectation maximisation, which includes likelihood maximisation and ordered subset maximisation.
- The simultaneous ART (SART) and ART are both included in the algebraic reconstruction approach [18].
- Parts of Bayesian reconstruction include max. a posteriori and sorted subsets max. posteriori, both of which use a unit step.
- Algorithms that are iterative.

Modern PET scanners made for tiny creatures

High-resolution scanners such as the Albira Si, which uses novel monolithic LYSO crystal technology to achieve 0.89 mm resolution, are the result of recent developments. Sadly, access limitations make it difficult to reveal the precise parameters that certain study teams use.
Scanner sensitivity and resolution have been transformed by iterative reconstruction approaches, leading to significant improvements. The average absolute sensitivity is around 5%, while some scanners have higher sensitivity levels. For example, the Sofie G8, UCLA PETBox4, and Molecubes cubes have all shown remarkable sensitivity performance. To increase sensitivity, researchers use a variety of techniques, such as enhancing the line segment that extends from the geometric origin. Scintillators with high stopping power may also be used judiciously to boost sensitivity.

III. METHODOLOGY

The following tactics were used to get the desired result:

- Utilise the Geant4 application.
- Utilise C++ abilities or instructions.
- Create PET/SPECT phantoms using Nema's Geant4 software.
- Make PET/SPECT models for the experiment using Geant4 (Nema).
- PET/ SPET detector

Small Animal Phantom NEMA PET (NU 4, 2008)

constructed to satisfy the requirements for developing PET performance metrics in animal imaging given out by the NEMA (Fig. 2).

Fig. 2. NEMA PET's animal phantom (NU 4-2008)

Features

TABLE 1. MEASURABLE FEATURES

Parameter	Value (mm)
Distance from the centre	18.00
Length of Cylinder	65.00
Diameter of the Interior of the Fillable Chamber	32.00
Length of Fillable Chamber	2.20
Sidewall Thickness	2.20
The fillable chamber's inner radius	4.60
Length of Fillable Chamber Inside	15.50
Thickness of filled chamber wall	1.60
The Dimensions of the Hot Spots :	
Length	21.00
radii	0.6, 1.1, 1.6, 2.1, and 2.6

NEMA PET Phantom Generation in Geant4

The phantom's dimensions, which were created using Geant4, are summarised here. Figure 3 displays the NEMA Phantom application in Geant 4.

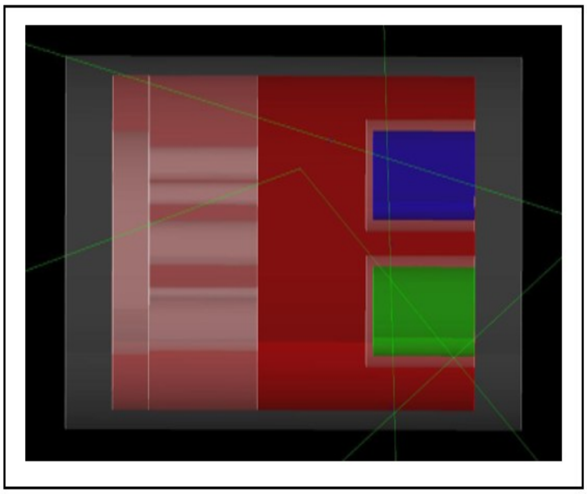

Fig. 3. Application of NEMA Phantom

It is important to know the following:

- The straight LOR for photon destruction at 511 keV is shown green.
- The scattering curve shows a reaction which doesn't follow a straight line.

IV. EXPERIMENTAL FINDINDS

PET/Single Photon Emission CT Detector

Fig. 4 shows a Geant 4 monolithic crystalline detector with SiPMs and a Nema NU-2008 phantom.

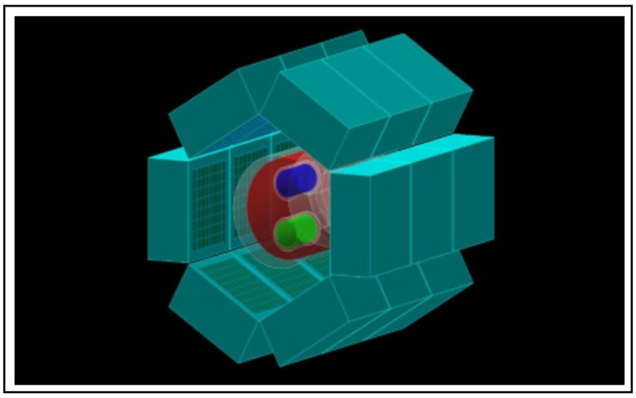

Fig. 4. PET/SPECT Detector

Geant4-simulated detector has characteristics that are comparable to those of the NEMA Phantom 2008:

- multiple modes,
- monolithic design
- SiPMs
- FSR
- Not very dense
- plastic path for light

Executing Geant4 Phantoms:

- NEMA-NU 2008

Attenuation PET/SPECT Modes

LYSO scintillation detector has an attenuation length = 1.15 cm (11.6 mm) for 511 keV PET and 0.15 cm (1.5 mm) for 140 keV SPECT.

FSR Vs BSR

Annihilation photon beam may be changed by placing a SiPM array on the crystal's front surface, ensuring a better FSR than BSR. Approximately 60% of the annihilation light passes through the front region of the crystal's surface. Moreover, as issues occur close to the SiPM matrix, the light dispersions exhibit greater skewness as well as variableness proportional to the interaction location. Fig. 5 depicts the geometric forms of the FSR/BSR.

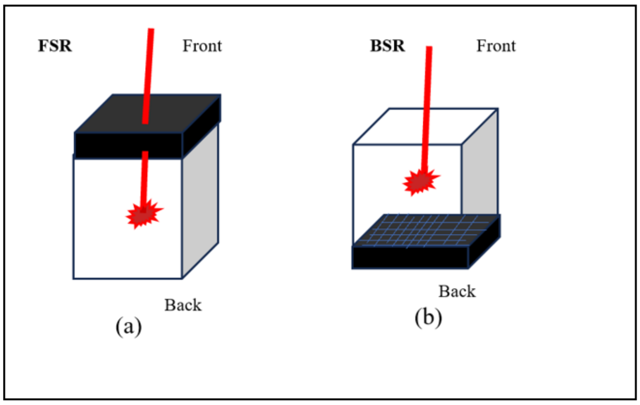

Fig. 5. Geometrical shapes of (a) FSR and (b) BSR

Unlike BSR, the LYSO scintillator requires FSR to improve photon detection efficiency since the front side collects more photons per SiPM pixel [19].

Many aspects should be considered while designing SPECT systems.

Due to limitations in photon attenuation length, SiPMs with a FSR are preferred over those with a BSR.

Due to internal reflection, tight contact sites with the SiPMs matrix limit resolution to 3 mm, affecting depth absorption distribution. Light guides with 0.5 mm radii [20].

V. DISCUSSIONS

The positron's range while annihilating an electron is determined by its energy and interactions with nearby materials. Two 511-keV photons go in opposing directions. Within a ring of detectors around the radiation source, PET scanner detectors record all simultaneous events in a certain time period. The monolithic scintillator technique was chosen due to its simple manufacturing process and absence of the need for additional SiPMs.

Geant4 has produced a variety of physics-related packages, including the G4EmStandardPhysics option4 constructor. This constructor is used to build the physics basis. Photons interact with matter by a variety of electromagnetic processes, including Compton dispersion, Rayleigh dispersion, and photoelectric absorption, all of which have a substantial influence on their behaviour. When performing PET at 511 keV, the LYSO scintillation detector has an attenuation length = 1.15 cm. At 140 keV, the attenuation length = 0.15 cm.

VI. CONCLUSION

Geant4 shows the below mentioned properties for a joint detector employing SiPMs: multimodal, monolithic, FSR, SiPMs, small density, along with a plastic light guide. The PET absorption length = 1.15 cm and the SPECT 0.16 cm. As a result, for SiPMs, we use the LSYO detector's FSR feature. The above-mentioned collaborative detector for PET/SPECT has the benefit of radiation sensitivity, and the pattern in Geant4 is an implementation of it. The research must be recognised in current times in order to improve the gamma camera's detecting performance. This would also help us avoid radiation impacts on patients during scans.

REFERENCES

[1] M.M. Khalil (Ed.). Basic sciences of nuclear medicine. Springer Nature, 2021.

[2] G. F. Knoll, "Radiation Detection and Measurement," 4th ed., Wiley, 2010.

[3] J. Xie, H. Wang, S. Merzi, G. Paternoster, A. Gola, J. Qi, S.R. Cherry, and J. Du, "High spatial resolution PET detectors based on 10 mm× 10 mm linearly-graded SiPMs and 0.5 mm pitch LYSO arrays," Physics in Medicine & Biology, 70(2), 025016, 2025.

[4] P. Hallen, D. Schug, & V. Schulz, "Comments on the NEMA NU 4-2008 standard on performance measurement of small animal positron emission tomographs," EJNMMI physics, 7(1), 12, 2020.

[5] S. R. Cherry, J.A. Sorenson, M.E. Phelps, & ScienceDirect (Online service). Physics in nuclear medicine (Vol. 3). Saunders, 2023.

[6] T. Gupta, "Radiation, ionization, and detection in nuclear medicine," Heidelberg: Springer, pp. 451-494, 2013.

[7] G. Crișan, N.S. Moldovean-Cioroianu, D.G. Timaru, G. Andrieș, C. Căinap, & V. Chiș, Radiopharmaceuticals for PET and SPECT imaging: a literature review over the last decade. International journal of molecular sciences, 23(9), 5023, 2022.

[8] L. Semeraro, V. Frantellizzi, L. Filippi, B. Palumbo, G. De Vincentis, & M. S. De Feo, "Positron Emission Tomography with Fibroblast Activation Protein-Targeted Radiopharmaceuticals in Primary Hepatic Tumors: A Systematic Review," Applied Sciences, 15(4), 2025.

[9] S. Hatefi Hesari, M. A. Haque, & N. McFarlane, "A comprehensive survey of readout strategies for SiPMs used in nuclear imaging systems. In Photonics, Vol. 8, No. 7, p. 266, MDPI, 2021.

[10] N. Takahashi, T. Inoue, J. Lee, T. Yamaguchi, & K. Shizukuishi, "The roles of PET and PET/CT in the diagnosis and management of prostate cancer. Oncology, 72(3-4), pp. 226-233, 2008.

[11] W. A. Weber, M. Schwaiger, & N. Avril, "Quantitative assessment of tumor metabolism using FDG-PET imaging. Nuclear medicine and biology, 27(7), pp. 683-687, 2000.

[12] I. Mbutu-Austin, B. Modarai, E. Ainsbury, & S. Y. Terry, "Potential biomarkers of chronic low-dose radiation exposure for nuclear medicine technologists," International Journal of Radiation Biology, 101(5), pp.453-466.

[13] C. Vanhove, M. Koole, P. Fragoso Costa, M. Schottelius, J. Mannheim, C. Kuntner,... & M. Bernsen, "Preclinical SPECT and PET: joint EANM and ESMI procedure guideline for implementing an efficient quality control programme. European Journal of Nuclear Medicine and Molecular Imaging, 51(13), pp. 3822-3839, 2024.

[14] N. Vahidfar, M.B. Kashi, S. Afshar, P. Sheikhzadeh, S. Farzanefar, Y. Salehi, ... & E. Eppard, "Recent advances of copper-64 based radiopharmaceuticals in nuclear medicine," Advances in dosimetry and new trends in radiopharmaceuticals, 2024.

[15] N. Robson, & D. K. Thekkinkattil, "Current role and future prospects of positron emission tomography (PET)/computed tomography (CT) in the management of breast cancer," Medicina, 60(2), 321, 2024.

[16] W. Tapper, G. Carneiro, C. Mikropoulos, S.A. Thomas, P. M., Evans, & S. Boussios, "The application of radiomics and AI to molecular imaging for prostate cancer," Journal of personalized medicine, *14*(3), 287, 2024.

[17] F. Hashimoto, Y. Onishi, K. Ote, H. Tashima, A. J. Reader, & T. Yamaya, "Deep learning-based PET image denoising and reconstruction: a review," Radiological physics and technology, 17(1), pp. 24-46, 2024.

[18] B. Abhisheka, S. K. Biswas, B. Purkayastha, D. Das, & A. Escargueil, "Recent trend in medical imaging modalities and their applications in disease diagnosis: a review," Multimedia Tools and Applications, 83(14), pp. 43035-43070, 2024.

[19] A. Boudjelal, Z. Messali, A. Elmoataz, & B. Attallah, "Improved simultaneous algebraic reconstruction technique algorithm for positron-emission tomography image reconstruction via minimizing the fast total variation," Journal of medical imaging and radiation sciences, 48(4), pp. 385-393, 2017.

[20] P. J. Green, "Bayesian reconstructions from emission tomography data using a modified EM algorithm. IEEE transactions on medical imaging, 9(1), pp. 84-93, 1990.